nature medicine

ARTICLES

VEGF modulates erythropoiesis through regulation of adult hepatic erythropoietin synthesis

Betty Y Y Tam[1,10,11], Kevin Wei[1,11], John S Rudge[2], Jana Hoffman[1], Joceyln Holash[2], Sang-ki Park[3,10], Jenny Yuan[1], Colleen Hefner[4], Cecile Chartier[1], Jeng-Shin Lee[5], Shelly Jiang[2], Nihar R Niyak[6], Frans A Kuypers[7], Lisa Ma[1], Uma Sundram[8], Grace Wu[1], Joseph A Garcia[9], Stanley L Schrier[1], Jacquelyn J Maher[4], Randall S Johnson[3], George D Yancopoulos[2], Richard C Mulligan[5] & Calvin J Kuo[1]

Vascular endothelial growth factor (VEGF) exerts crucial functions during pathological angiogenesis and normal physiology. We observed increased hematocrit (60–75%) after high-grade inhibition of VEGF by diverse methods, including adenoviral expression of soluble VEGF receptor (VEGFR) ectodomains, recombinant VEGF Trap protein and the VEGFR2-selective antibody DC101. Increased production of red blood cells (erythrocytosis) occurred in both mouse and primate models, and was associated with near-complete neutralization of VEGF corneal micropocket angiogenesis. High-grade inhibition of VEGF induced hepatic synthesis of erythropoietin (Epo, encoded by *Epo*) >40-fold through a HIF-1α–independent mechanism, in parallel with suppression of renal *Epo* mRNA. Studies using hepatocyte-specific deletion of the *Vegfa* gene and hepatocyte–endothelial cell cocultures indicated that blockade of VEGF induced hepatic *Epo* by interfering with homeostatic VEGFR2-dependent paracrine signaling involving interactions between hepatocytes and endothelial cells. These data indicate that VEGF is a previously unsuspected negative regulator of hepatic *Epo* synthesis and erythropoiesis and suggest that levels of Epo and erythrocytosis could represent noninvasive surrogate markers for stringent blockade of VEGF *in vivo*.

VEGF serves essential functions during both physiological and pathological angiogenesis, and has been the target of many therapeutics for cancer and ocular disorders[1–4]. Efforts towards uncovering VEGF functions during adult physiology have been impeded by the embryonic lethality of embryos lacking either VEGF or VEGFRs[5]. Alternatively, pharmacologic VEGF inhibitors such as antibodies specific for VEGF, soluble VEGFRs and small-molecule antagonists of the VEGFR tyrosine kinase domains[3,6–8] have led to the discovery of VEGF functions in processes such as corpus luteum angiogenesis, bone formation, collateral formation, glomerular permeability and preeclampsia[5,9–12]. These functions of VEGF in the adult are relevant to the identification of dose-limiting clinical toxicities for VEGF inhibition, as exemplified by the concordance of proteinuria and hypertension in animals and humans treated with VEGF inhibitors[9,13].

We previously generated adenoviruses expressing ligand-binding soluble extracellular domains of VEGFRs (Ad-sVEGFRs), including the Flk1 (the human version of which is also named KDR or VEGFR2) or Flt1 (the human version of which is also named VEGFR1) ectodomains, and VEGF Trap[3,6,8], a fusion of the VEGF binding domains of Flk1 and Flt1 that is currently in human clinical trials[4]. A single intravenous administration of Ad-sVEGFRs produces highly selective hepatic infection, accompanied by high-level and continuous ectodomain secretion into the circulation for several weeks, potent conditional inactivation of VEGF function and systemic inhibition of tumor angiogenesis[6,11,14]. Here, adenoviral expression of VEGF Trap, Flk1 or Flt1 ectodomains, or treatment with recombinant VEGF Trap or the VEGFR2-selective monoclonal antibody DC101 (ref. 15), produced erythrocytosis in both mouse and primate models, increasing hematocrit to 75% (versus basal levels of ~45%). This erythrocytosis correlated with near-complete inhibition of VEGF in corneal micropocket assays, and with induction of hepatic transcription of *Epo*. These data suggest that VEGF functions physiologically to repress hepatic synthesis of *Epo* and that adult hepatocytes retain a latent capacity for production of Epo through a HIF-1α–independent pathway dependent on VEGFR2. Additionally, these studies identify erythrocytosis as a potential surrogate marker for extremely stringent

[1]Division of Hematology, Stanford University School of Medicine, 269 Campus Drive, CCSR 1155, Stanford, California, 94305, USA. [2]Regeneron Pharmaceuticals, Incorporated, 777 Old Saw Mill River Road, Tarrytown, New York 10591, USA. [3]University of California, San Diego, Molecular Biology Section, Division of Biological Sciences, 9500 Gilman Drive, La Jolla, California 92093, USA. [4]Liver Center and Department of Medicine, S-357 University of California, San Francisco, California 94143, USA. [5]Department of Genetics, Harvard Medical School, Division of Molecular Medicine, Children's Hospital, 300 Longwood Avenue, Boston, Massachusetts 02115, USA. [6]Division of Gynecology and Obstetrics, Stanford University School of Medicine, 300 Pasteur Drive, Stanford, California 94305, USA. [7]Children's Hospital Oakland Research Institute, 5700 Martin Luther King Jr. Way, Oakland, California 94609, USA. [8]Division of Pathology, Stanford University School of Medicine, 300 Pasteur Drive, Stanford, California 94305, USA. [9]University of Texas Southwestern Medical Center at Dallas, Division of Cardiology MC8573, 5323 Harry Hines Boulevard, Dallas, Texas 75390, USA. [10]Present addresses: TargeGen Inc., 9380 Judicial Drive, San Diego, California 92121, USA (B.Y.Y.T.) and Department of Pharmaceutical Sciences, St. John's University, 8000 Utopia Parkway, Queens, New York 11438, USA (S.-K.P.). [11]These authors contributed equally to this work. Correspondence should be addressed to C.J.K. (cjkuo@stanford.edu).

Received 20 February; accepted 3 May; published online 25 June 2006; doi:10.1038/nm1428

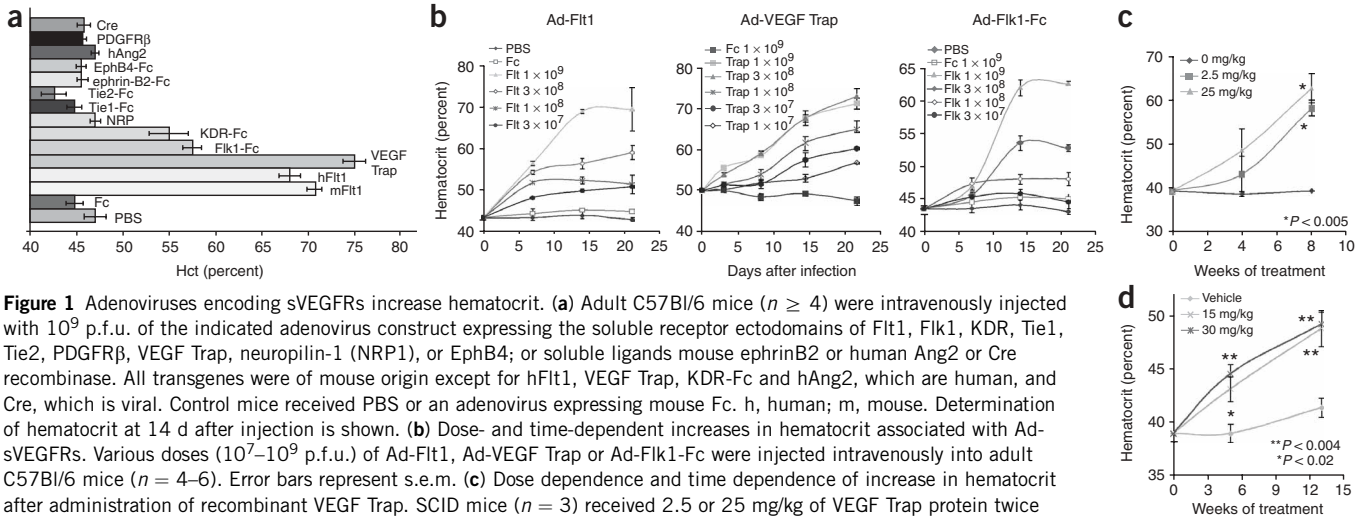

Figure 1 Adenoviruses encoding sVEGFRs increase hematocrit. (**a**) Adult C57Bl/6 mice ($n \geq 4$) were intravenously injected with 10^9 p.f.u. of the indicated adenovirus construct expressing the soluble receptor ectodomains of Flt1, Flk1, KDR, Tie1, Tie2, PDGFRβ, VEGF Trap, neuropilin-1 (NRP1), or EphB4; or soluble ligands mouse ephrinB2 or human Ang2 or Cre recombinase. All transgenes were of mouse origin except for hFlt1, VEGF Trap, KDR-Fc and hAng2, which are human, and Cre, which is viral. Control mice received PBS or an adenovirus expressing mouse Fc. h, human; m, mouse. Determination of hematocrit at 14 d after injection is shown. (**b**) Dose- and time-dependent increases in hematocrit associated with Ad-sVEGFRs. Various doses (10^7–10^9 p.f.u.) of Ad-Flt1, Ad-VEGF Trap or Ad-Flk1-Fc were injected intravenously into adult C57Bl/6 mice ($n = 4$–6). Error bars represent s.e.m. (**c**) Dose dependence and time dependence of increase in hematocrit after administration of recombinant VEGF Trap. SCID mice ($n = 3$) received 2.5 or 25 mg/kg of VEGF Trap protein twice weekly subcutaneously. (**d**) Increased hematocrit at 13 weeks in monkeys ($n = 6$) treated subcutaneously twice weekly with 15 or 30 mg/kg of VEGF Trap protein. Error bars represent s.e.m.

blockade of VEGF, relevant to the numerous VEGF-targeted agents currently in human dose-escalation studies[3,4,16].

RESULTS

Adenoviruses encoding sVEGFRs increase hematocrit

Single intravenous injections of adenoviruses expressing soluble ectodomains of the VEGF receptors Flk1 and Flt1 (Ad-Flk1-Fc and Ad-Flt1, respectively) transduce the liver, with hepatic secretion of circulating receptor for >3 weeks and systemic inhibition of tumor angiogenesis[6]. Non–tumor-bearing adult mice (C57Bl/6 mice, 10–16 weeks old) infected with adenovirus expressing mouse Flt1 ectodomain or the lower-affinity receptor Flk1-Fc unexpectedly showed markedly elevated hematocrit (58–70%) by 14 d compared with normal hematocrit (~45%) for controls receiving phosphate-buffered saline (PBS) or Ad-Fc, which encodes a mouse immunoglobulin IgG2α Fc fragment (**Fig. 1a**). Elevated hematocrit also developed with adenoviruses expressing soluble ectodomains of the human VEGFRs hFlt1 (Ad-hFlt1; 68%), KDR (Ad-KDR-Fc; 55%) or the recently described hFlt1-KDR hybrid ectodomain VEGF Trap[8] (Ad-VEGF Trap; 74%), but not with a panel of control adenoviruses encoding Cre recombinase or the soluble ectodomains of other endothelial or angiogenesis-related receptors including Tie1, Tie2, ephrin-B2, EphB4, neuropilin-1 and platelet-derived growth factor receptor (**Fig. 1a**).

Delivery of Ad-sVEGFRs increased hematocrit in a dose- and time-dependent manner (**Fig. 1b**). Injection of high doses (3×10^8–3×10^9 plaque-forming units (p.f.u.)) of Ad-Flt1 or Ad-VEGF Trap led to the accumulation of clear peritoneal ascites in some mice and the death of several mice between 25 d and 85 d after vector administration, which was not observed with the lower-affinity Flk1 ectodomain. This toxicity, previously reported for Ad-Flt1 (ref. 6), seems to be dependent upon the delivery of soluble VEGFRs through adenoviral vectors, as no such effects have been observed with the injection of high doses of VEGF Trap protein.

Recombinant VEGF Trap increases hematocrit

As an alternative nonviral method of VEGF blockade, 7-week-old mice with severe combined immunodeficiency (SCID) received subcutaneous injections of recombinant VEGF Trap at 2.5 and 25 mg/kg twice weekly, producing significant dose- and time-dependent increases in hematocrit to ~62% ($P < 0.005$; **Fig. 1c**). We observed identical effects with 13–15-week-old SCID mice, and thrice-weekly dosing produced more rapid and profound increases in hematocrit (data not

Table 1 Selective erythrocytosis with minimal alteration in WBC and platelet levels after treatment with diverse VEGF inhibitors

	RBC (10^6/ml)	WBC (10^3/ml)	Platelets (10^3/ml)	Hematocrit (percent)
C57Bl/6				
PBS	9.1 ± 0.3	7.5 ± 0.9	1,240 ± 74	46.8 ± 0.8
Ad-Fc	8.9 ± 0.2	9.3 ± 0.8	1,435 ± 35	48.4 ± 0.7
Ad-Flt1	13.7 ± 0.2 *	8.9 ± 0.6	1,372 ± 78	69.4 ± 1.0 *
Ad-VEGF Trap	13.9 ± 0.1 *	10.4 ± 0.8	1,285 ± 88	67.0 ± 1.3 *
Ad-Flk1-Fc	11.6 ± 0.2 *	9.3 ± 0.7	1,013 ± 37*	61.3 ± 0.6 *
SCID				
Vehicle	8.4 ± 0.5	1.0 ± 0.2	1,043 ± 92	41.0 ± 2.8
rVEGF Trap	10.7 ± 0.5 **	1.2 ± 0.5	1,004 ± 94	56.4 ± 2.7 **
DC101	11.7 ± 0.8 ***	1.1 ± 0.4	842 ± 80 ***	59.2 ± 3.3 ***
C57Bl/6				
Vehicle	9.2 ± 0.04	8.1 ± 1.1	ND	45.1 ± 0.6
ZD4190	9.9 ± 0.2 ‡	5.3 ± 1.6	ND	48.5 ± 0.5 ‡

Adult C57Bl/6 mice received a single intravenous injection of Ad-Flt1 or Ad-Flk1 (10^9 p.f.u., $n = 5$), Ad-VEGF Trap (3×10^8 p.f.u., $n = 5$), ZD4190 in PBS containing 0.1% Tween-80 (100 mg/kg/d orally, $n = 5$) or 0.1% Tween-80 vehicle control ($n = 6$) followed by automated CBC determination after 14 d. Similarly, adult SCID mice received recombinant VEGF Trap (5 mg/kg subcutaneous twice weekly, $n = 8$) or the VEGFR2-specific monoclonal antibody DC101 (40 mg/kg subcutaneously twice weekly, $n = 4$) or vehicle ($n = 10$) followed by automated CBC determination after 8 weeks. Error ranges represent s.e.m. ND, not determined.
*$P < 0.000001$ versus Fc, ** $P < 0.00000001$ versus vehicle, *** $P < 0.003$ versus vehicle, ‡ $P < 0.015$ versus vehicle.

Table 2 Elevated hematocrit is associated with stringent VEGF blockade

Virus	Dose (p.f.u.)	Day 3 plasma level (mg/ml)	Percent inhibition in cornea assay	Hematocrit at day 14 after infection (percent)
Fc	1×10^9	–	0	47 ± 0.8
	1×10^9	0.0085 ± 0.0006	99.3 ± 0.5	65 ± 1.1
	3×10^8	0.0032 ± 0.0009	99.2 ± 0.5	64 ± 1.9
Flt1	1×10^8	0.001 ± 0.0003	96.1 ± 1.7	55.5 ± 0.7
	3×10^7	0.00006 ± 0.0004	96.1 ± 5.5	49.5 ± 0.6
	1×10^6	ND	45 ± 12.3	47.7 ± 0.3
	1×10^9	14.4 ± 1.4	100	67.7 ± 1.5
	3×10^8	5.6 ± 1.2	99.1 ± 1.4	66.5 ± 0.9
	1×10^8	1.9 ± 0.3	97.1 ± 1.4	62.6 ± 0.6
VEGF Trap	3×10^7	0.3 ± 0.1	93.2 ± 2.6	59 ± 1.2
	1×10^7	0.08 ± 0.003	93.3 ± 3.9	52 ± 0.9
	3×10^6	0.002 ± 0.0009	48.1 ± 8.2	48.7 ± 0.7
	1×10^6	0.003 ± 0.0003	19.4 ± 8.9	48.4 ± 0.9
	1×10^9	3.3 ± 1.0	97.3 ± 1.1	56 ± 0.1
	3×10^8	0.2 ± 0.05	93.9 ± 0.7	54 ± 0.7
Flk1-Fc	1×10^8	0.017 ± 0.003	77 ± 3.9	50.2 ± 0.3
	3×10^7	0.002 ± 0.0008	43.8 ± 6.4	48.7 ± 0.7
	1×10^6	ND	23.5 ± 4.9	48.3 ± 0.9

Adult C57Bl/6 mice were injected intravenously with various doses of Ad-Flt1, Ad-VEGF Trap or Ad-Flk1-Fc or 10^9 p.f.u. of the negative control virus Ad-Fc ($n = 4$). Two days after injection, the same mice received corneal implantation of a slow-release hydron VEGF pellet for the corneal micropocket angiogenesis assay as described[6]. Corneal neovascularization was quantified 6 d after pellet implantation, showing dose-dependent inhibition of angiogenesis. Hematocrit was measured in the same mice 14 d after original adenovirus administration, and marked hematocrit increases were generally present only in mice with >93% inhibition of VEGF-induced corneal neovascularization. Error ranges represent s.e.m. ND, not determined.

shown). Treatment of cynomolgus monkeys with recombinant VEGF Trap at 15–30 mg/kg subcutaneously twice weekly resulted in more modest but significant ~10% increases in hematocrit to 49% by 13 weeks of treatment ($P < 0.004$; **Fig. 1d**), suggesting conservation of this effect amongst vertebrates. Furthermore, increases in hematocrit were reversible, as hematocrit returned to normal levels within 4 weeks of cessation of recombinant VEGF Trap dosing in preliminary studies with 15-week-old SCID mice treated with similar doses (data not shown). In the studies described, chronic treatment with recombinant VEGF Trap was not associated with lethality in mice or monkeys, even at weekly cumulative doses of 120 mg/kg subcutaneously.

VEGF blockade induces selective erythrocytosis

Both Ad-sVEGFRs or recombinant VEGF Trap strongly increased red blood cell (RBC) number and hematocrit, whereas white blood cell (WBC) count and platelet number remained generally unaltered (**Table 1**). Small increases in WBC numbers in adenovirus-treated mice (including treatment with Ad-Fc) compared to PBS-treated mice were probably related to the immune response elicited by adenoviral infection. Notably, the VEGFR2-selective monoclonal antibody DC101 (ref. 15; 40 mg/kg subcutaneously, twice weekly) also increased hematocrit from basal levels of 41% to treatment levels of 59% ($P < 0.003$; **Table 1**), consistent with the involvement of Flk1. The small-molecule VEGFR antagonist ZD4190 (ref. 17) administered at 100 mg/kg/d orally for 14 d produced minor but statistically significant increases in RBC number and hematocrit (45–48%; $P < 0.015$; **Table 1**). We also observed decreased platelet number and WBC count with DC101 and ZD4190, respectively, but not consistently with soluble VEGFRs, suggesting possible off-target effects.

Ad-Flt1, Ad-VEGF Trap and Ad-Flk1-Fc but not Ad-Fc transiently elevated the peripheral blood reticulocyte index (**Supplementary Fig. 1** online). Ad-sVEGFRs increased splenic and bone marrow $Ter119^+CD45^-$ erythroid precursors and colony-forming units–erythroid (CFU-E) progenitors similar to an adenovirus expressing macaque monkey erythropoietin (Ad-mac Epo), whereas treatment with Ad-Flt1 markedly elevated RBC mass as measured by RBC biotinylation (**Supplementary Fig. 1** and **Supplementary Table 1** online). Determination of serum blood urea nitrogen/creatinine ratios

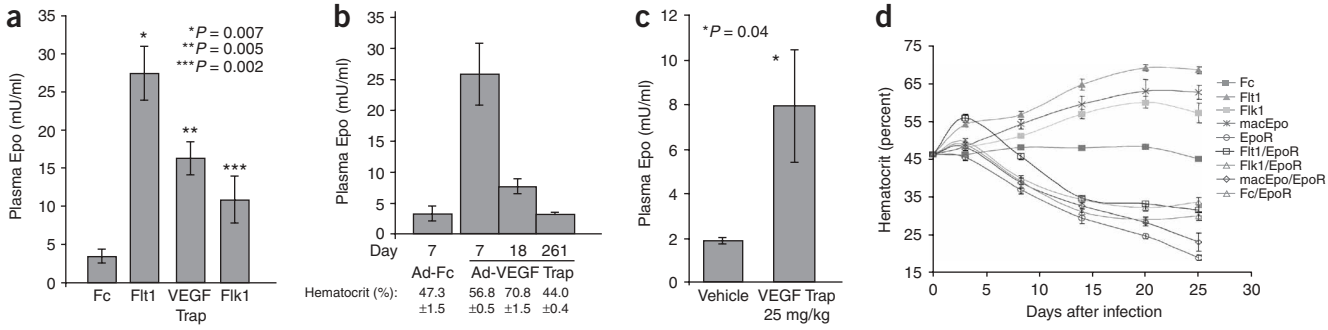

Figure 2 High-grade inhibition of VEGF induces production of Epo. (**a**) Increased plasma Epo after Ad-sVEGFR treatment. Adult C57Bl/6 male mice ($n = 10$) received a single intravenous administration of PBS or 10^9 p.f.u. of indicated viruses, followed by determination of plasma Epo at 21 d. (**b**) Reversibility of increased plasma Epo after a single intravenous injection of 3×10^8 p.f.u. Ad-Fc or Ad-VEGF Trap in adult C57Bl/6 mice ($n = 4$). (**c**) Recombinant VEGF Trap increases plasma Epo. Seven-week-old male SCID mice ($n = 6$) received 25 mg/kg subcutaneous injections of recombinant VEGF Trap three times per week followed by ELISA determination of plasma Epo at 28 d. (**d**) Antagonism of Ad-sVEGFR–induced erythrocytosis by Ad-EpoR-Fc. Adult C57Bl/6 mice ($n = 5$) received an intravenous injection of 10^9 p.f.u. of the indicated viruses alone or in combination with Ad-EpoR-Fc (~2×10^7 p.f.u.), except for Ad-mac Epo, which was administered at 10^5 p.f.u. Ad-EpoR-Fc was sufficient to abrogate the erythrocytosis induced by either Ad-sVEGFRs or Ad-mac Epo. Error bars represent s.e.m.

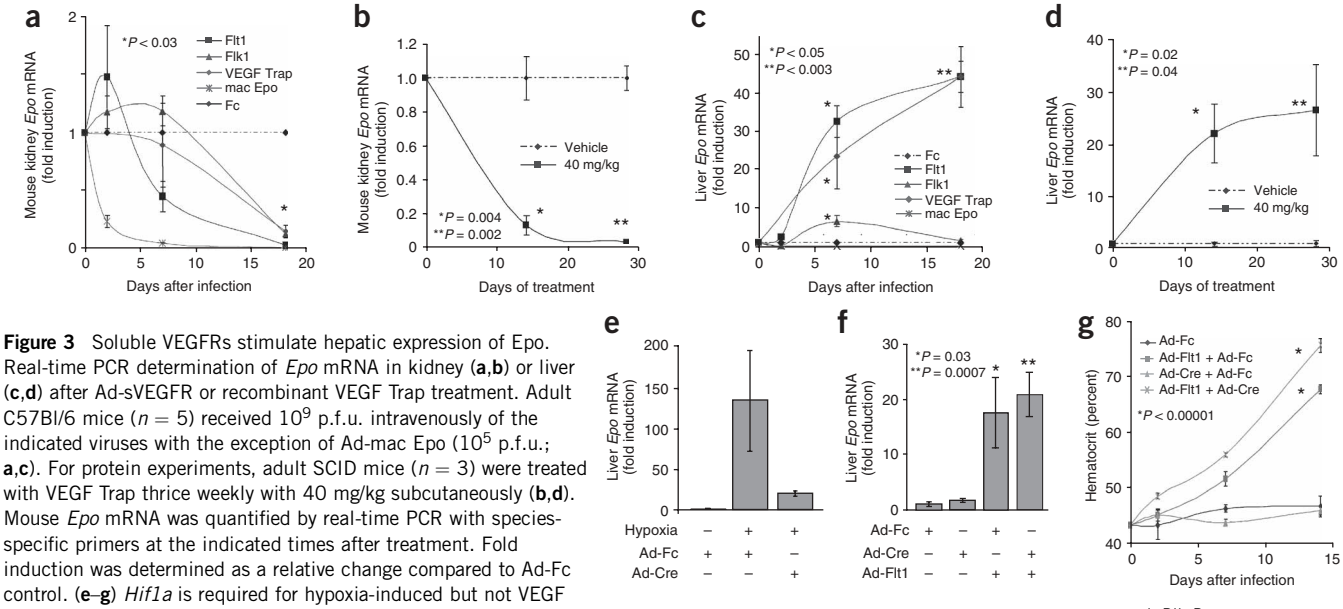

Figure 3 Soluble VEGFRs stimulate hepatic expression of Epo. Real-time PCR determination of *Epo* mRNA in kidney (**a**,**b**) or liver (**c**,**d**) after Ad-sVEGFR or recombinant VEGF Trap treatment. Adult C57Bl/6 mice ($n = 5$) received 10^9 p.f.u. intravenously of the indicated viruses with the exception of Ad-mac Epo (10^5 p.f.u.; **a**,**c**). For protein experiments, adult SCID mice ($n = 3$) were treated with VEGF Trap thrice weekly with 40 mg/kg subcutaneously (**b**,**d**). Mouse *Epo* mRNA was quantified by real-time PCR with species-specific primers at the indicated times after treatment. Fold induction was determined as a relative change compared to Ad-Fc control. (**e**–**g**) *Hif1a* is required for hypoxia-induced but not VEGF blockade–induced hepatic production of Epo. (**e**) Impairment of hypoxia-induced hepatic *Epo* synthesis by Ad-Cre treatment of $Hif1a^{loxP/loxP}$ mice. Adult $Hif1a^{loxP/loxP}$ mice ($n = 4$) received a single intravenous injection of 5×10^8 p.f.u. Ad-Cre or Ad-Fc. After 10 d, mice were placed in a hypoxia chamber (7.5% O_2) for 6 h followed by real-time PCR determination of hepatic *Epo* mRNA. (**f**,**g**) $Hif1a^{loxP/loxP}$ mice ($n = 5$) were injected with Ad-Fc (10^9 p.f.u.) or a combination of Ad-Fc and Ad-Cre or Ad-Flt1 and Ad-Cre (5×10^8 p.f.u. each). Ad-Cre–mediated excision of *Hif1a* in liver did not inhibit the increase in hepatic Epo message levels at 14 d after infection versus Ad-Flt1 controls (**f**) or Ad-Flt1–mediated elevation of hematocrit (**g**). Error bars represent s.e.m.

and arterial pO_2 in these mice did not show evidence of dehydration or systemic hypoxemia, ruling these out as possible causes of spurious or secondary hematocrit elevation (**Supplementary Table 2** online), and colony-forming units–granulocyte-macrophage (CFU-GM) and peripheral blood T-cell counts were unaffected (data not shown).

Erythrocytosis is associated with stringent VEGF blockade

To examine the relationship between the degree of erythrocytosis and the degree of systemic blockade of VEGF, we performed simultaneous determination of hematocrit and VEGF-induced corneal micropocket angiogenesis in mice after a single intravenous injection of Ad-sVEGFRs. We saw prominent increases in hematocrit only with near-complete suppression of VEGF-dependent corneal micropocket angiogenesis (**Table 2**), suggesting a requirement for stringent *in vivo* blockade of VEGF. The peak day 3 plasma sVEGFR levels correlating with half-maximal corneal VEGF inhibition were <60 ng/ml for Ad-Flt1 and ~3 μg/ml for Ad-VEGF Trap and Ad-Flk1-Fc, respectively (**Table 2**). The tendency of Flt1 to bind to extracellular matrix[6,8] is likely to result in its deposition in tissues, particularly at its site of synthesis in the liver, accounting for its low circulating levels and its efficacy at these levels.

Plasma Epo induction after high-grade inhibition of VEGF

PBS- and Ad-Fc–treated adult C57Bl/6 mice had basal plasma Epo levels of 0–4 mU/ml (**Fig. 2a**) as determined by mouse Epo ELISA[18]. But plasma Epo levels were significantly elevated by Ad-Flt1 (27.5 mU/ml, $P = 0.007$), Ad-VEGF Trap (16.4 mU/ml, $P = 0.005$) and Ad-Flk1-Fc (10.9 mU/ml, $P = 0.002$) by 21 d (**Fig. 2a**) or 7 d (data not shown). These elevations in plasma Epo were reversible (**Fig. 2b**), and recombinant VEGF Trap also elevated plasma Epo in SCID mice (8.0 mU/ml, $P = 0.04$; **Fig. 2c**).

VEGFRs are expressed on hematopoietic stem cells (HSCs)[19,20]. To exclude a direct, Epo-independent effect of VEGF blockade on HSC VEGFRs, we neutralized Epo *in vivo* using an adenovirus expressing a soluble Epo receptor–Fc fusion (Ad-EpoR-Fc; B.T. & C.J.K., unpublished data). Treatment of naive mice with Ad-EpoR-Fc produced progressive anemia with a decrease in hematocrit from 45% to 25% after 20 d, consistent with potent conditional Epo inactivation (**Fig. 2d**). Ad-Flt1, Ad-Flk1-Fc or Ad-mac Epo were unable to overcome Ad-EpoR-Fc–induced anemia (**Fig. 2d**). These results, together with the elevated plasma Epo levels observed, are consistent with the idea that erythrocytosis caused by blockade of VEGF is dependent on Epo.

Blockade of VEGF induces hepatic expression of Epo

In the adult, renal synthesis of Epo predominates and is readily induced by hypoxia and anemia[21]. Ad-sVEGFRs (**Fig. 3a**) or recombinant VEGF Trap (**Fig. 3b**), however, did not induce steady-state levels of renal *Epo* mRNA despite marked erythrocytosis (Ad-Flt1 increased hematocrit to 75%; Ad-VEGF Trap increased hematocrit to 74%, Ad-Flk1-Fc increased hematocrit to 59% and recombinant VEGF Trap increased hematocrit to 75%) and elevated plasma Epo (**Fig. 2**). In fact, by 18–28 d, steady-state levels of renal *Epo* RNA were suppressed by >95% in mice treated with Ad-sVEGFRs (**Fig. 3a**) and recombinant VEGF Trap (**Fig. 3b**), consistent with physiologically appropriate suppression by erythrocytosis, and strongly suggesting an extrarenal origin of the elevated plasma Epo. Accordingly, Ad-mac Epo treatment, in which erythrocytosis occurs secondary to ectopic hepatic *Epo* production, suppressed renal *Epo* mRNA even more rapidly (**Fig. 3a**).

As *Epo* is expressed in the embryonic liver, we examined potential sVEGFR induction of hepatic *Epo* synthesis. Ad-Flt1 and Ad-VEGF Trap (**Fig. 3c**) and recombinant VEGF Trap (**Fig. 3d**) markedly elevated hepatic *Epo* mRNA (44-, 44- and 26-fold, respectively), with smaller elevations by Ad-Flk1-Fc (sevenfold, $P < 0.05$; **Fig. 3c**). Hepatic *Epo* mRNA persisted inappropriately over 18–28 d (the latest time points

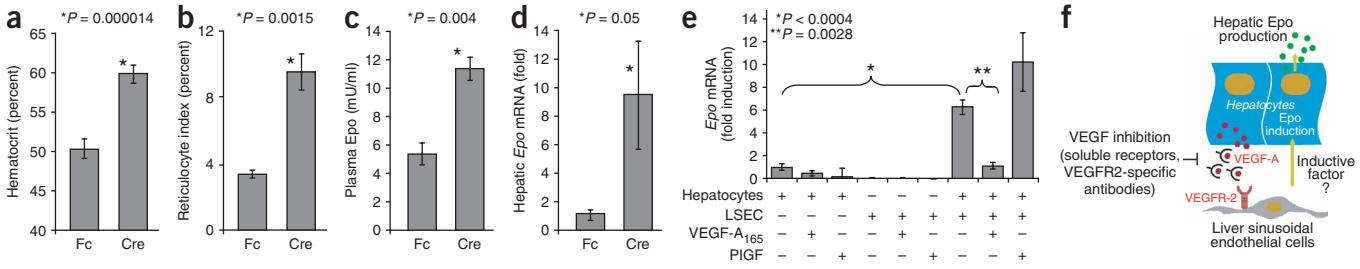

Figure 4 Elevated hematocrit and hepatic *Epo* mRNA in Ad-Cre–treated *Vegfa*$^{loxP/loxP}$ mice. Adult *Vegfa*$^{loxP/loxP}$ mice received a single intravenous injection of either Ad-Cre or Ad-Fc (10^9 p.f.u.). After 14 d, Ad-Cre–treated mice had increased hematocrit compared with Ad-Fc–treated mice ($n = 10$; **a**) and had reticulocytosis (**b**) and elevated plasma Epo (**c**) at 7 d ($n = 4$). (**d**) Stimulation of hepatic *Epo* mRNA at 14 d after infection in Ad-Cre–treated *Vegfa*$^{loxP/loxP}$ livers ($n = 4$). (**e**) Repression of hepatocyte *Epo* mRNA by VEGF-A in hepatocyte-LSEC coculture. Primary coculture of purified rat hepatocytes and LSECs was performed in the presence or absence or VEGF-A_{165} or PlGF, followed by real-time PCR quantification of hepatocyte Epo RNA at 3 d ($n = 6$ experiments). (**f**) Model. Hepatocyte-derived VEGF-A stimulates VEGFR2 on adjacent LSECs, leading to the lack of LSEC-derived factor(s) stimulating production of Epo by hepatocytes. Pharmacologic (soluble receptor, VEGFR2-specific antibody) or genetic (hepatocyte VEGF-A) deletion inhibits VEGFR2 on LSECs, resulting in active production of factor(s) by LSECs, which stimulate production of Epo by hepatocytes, with subsequent erythrocytosis. Error bars represent s.e.m.

evaluated) despite concomitant erythrocytosis, in contrast to complete suppression of renal *Epo* mRNA (**Fig. 3a**,**b**). *In situ* hybridization indicated that hepatocytes were the main cell type synthesizing *Epo* in Ad-Flt1–treated livers (**Supplementary Fig. 2** online), whereas nuclear run-on experiments confirmed a 23-fold increase in hepatic *Epo* transcription (data not shown). *Epo* mRNA was not elevated in Ad-sVEGFR–treated brain (data not shown).

Hepatic adenoviral infection was not needed for induction of *Epo*, as stimulation also occurred using recombinant VEGF Trap; however, we further excluded a requirement for hepatic adenoviral infection in Ad-sVEGFR–treated mice using parabiotic anastomosis in which the circulation of an Ad-Flt1–infected mouse was joined to that of a noninfected mouse. Under these conditions, hepatic *Epo* mRNA was induced in both the adenovirus-infected and noninfected livers, indicating independence from hepatic infection (**Supplementary Fig. 3** online). Similar increases in hepatic *Epo* mRNA were evident with intramuscular administration of Ad-VEGF Trap (B.T. & C.J.K., unpublished data). Induction of *Epo* resulting from chronic treatment with sVEGFRs contrasted with hypoxic (7.5% O_2) inductions of *Epo* mRNA in kidney and liver measured by quantitative RT-PCR, which were transient and were completely suppressed by 8–15 d (**Supplementary Fig. 4** online).

Stimulation of hepatic Epo is independent of HIF-1α

The central role of hypoxia and HIF-1α in regulation of Epo is well described[21]. To evaluate the role of HIF-1α (encoded by *Hif1a*) in sVEGFR-induced erythrocytosis, we selectively deleted *Hif1a* in hepatocytes of *Hif1a*$^{loxP/loxP}$ mice by *in vivo* treatment with adenovirus expressing Cre recombinase (Ad-Cre)[22]. Ad-Cre can elicit hepatocyte-specific, conditional deletion of floxed target genes after a single intravenous injection in adult mice[23] without infecting nonparenchymal cells such as endothelial cells or Kupffer cells[24,25]. We confirmed robust Ad-Cre–mediated excision of the *lox*P-flanked stop cassette in hepatocytes of *ROSA26-LacZ* mice[26] after 5 d, notably sparing the endothelium and nonparenchymal tissues (**Supplementary Fig. 5** online).

Ad-Cre treatment of *Hif1a*$^{loxP/loxP}$ mice produced up to 75% *Hif1a* gene excision in liver as assessed by real-time PCR of total liver genomic DNA, representing ~88% deletion of hepatocyte *Hif1a*, assuming that ~85% of cells in the liver are hepatocytes[27]. Hypoxia (7.5% O_2, 6 h)-stimulated expression of *Epo* in *Hif1a*$^{loxP/loxP}$ liver was inhibited by Ad-Cre but not Ad-Fc, consistent with HIF-1α being involved in hypoxic induction (**Fig. 3e**). In contrast, Ad-Cre did not inhibit Ad-Flt1–induced hepatic production of *Epo* or erythrocytosis in *Hif1a*$^{loxP/loxP}$ mice (**Fig. 3f**,**g**). Thus, deletion of *Hif1a* markedly impaired hypoxia-stimulated but not sVEGFR-stimulated hepatic expression of *Epo*.

Although we can not formally exclude a hypoxic mechanism, sVEGFR-treated liver did not exhibit staining with EF-5, a nitroimidazole derivative that specifically binds to hypoxic tissue adducts[28] (**Supplementary Fig. 6** online). Additionally, sVEGFR-treated liver showed neither histologic evidence of overt ischemic damage nor TUNEL-positive endothelial apoptosis, and mRNA levels of the hypoxia-regulated genes *Slc2a1* (encoding GLUT-1) and *Pgk1* (encoding phosphoglycerate kinase 1)[29] were not elevated (**Supplementary Fig. 7** online and data not shown).

Hepatocyte VEGF-A deletion induces erythrocytosis

Soluble VEGFRs could induce hepatic production of *Epo* by inhibiting either circulating VEGF produced by nonliver sources or local hepatocyte-produced VEGF; the importance of the latter has been recently described[30]. Treatment of *Vegfa*$^{loxP/loxP}$ mice[31] with Ad-Cre produced up to ~70% *Vegfa* gene deletion in hepatocytes, which was sufficient to increase hematocrit and induce reticulocytosis, serum Epo and hepatic *Epo* mRNA in Ad-Cre–treated versus Ad-Fc–treated *Vegfa*$^{loxP/loxP}$ mice (**Fig. 4a–d**). mRNA levels for the hypoxia-responsive *Slc2a1* and *Pgk1* genes were unaltered by deletion of VEGF in *Vegfa*$^{loxP/loxP}$ livers (data not shown). Consequently, loss of *Vegfa* in hepatocytes is sufficient to phenocopy induction of erythrocytosis and hepatic expression of Epo by sVEGFRs.

VEGF suppresses Epo in hepatocyte-LSEC coculture

The effects of hepatocyte *Vegfa* gene deletion on hepatic production of *Epo* mRNA could proceed either by cell-autonomous or non–cell-autonomous processes. The lack of VEGFR expression on hepatocytes[32,33], however, suggested the involvement of local hepatocyte-endothelium paracrine signaling, with hepatocyte-derived VEGF[34] acting through neighboring hepatic endothelial cells to suppress hepatic production of Epo. We examined this possibility by coculture of purified rat hepatocytes and liver sinusoidal endothelial cells (LSECs). Direct rat hepatocyte–LSEC coculture in the absence of exogenous VEGF resulted in >5-fold induction of *Epo* mRNA

(**Fig. 4e**); we saw identical results with coculture of mouse cells (**Supplementary Fig. 8** online). Notably, this induction was completely suppressed by recombinant VEGF-A_{165} but not the VEGFR1-selective ligand PlGF, consistent with regulation of *Epo* by VEGFR2 (**Fig. 4e**) and in agreement with the ability of the VEGFR2-selective monoclonal antibody DC101 to increase hematocrit *in vivo* (**Table 1**). Human umbilical vein endothelial cells (HUVECs), the pancreatic endothelial line MS1 and mouse embryonic fibroblasts were all ineffective in this coculture system (**Supplementary Fig. 8**), indicating a selective effect of the hepatic endothelium.

DISCUSSION

The definition of adult VEGF functions is relevant to both physiology and clinical VEGF inhibition, and has been greatly facilitated by pharmacologic VEGF inhibitors that phenocopy conditional VEGF inactivation and circumvent the embryonic lethality of VEGF- or VEGFR-knockout mice. Here, we used both soluble VEGFRs and antibodies specific to VEGFR2 to elicit a novel phenotype of erythrocytosis in both mice and primates. These data indicate that vertebrate erythropoiesis is negatively regulated by endogenous VEGF, and identify erythrocytosis and Epo as potential noninvasive markers for high-grade inhibition of VEGF *in vivo*.

Extremely stringent, near-complete blockade of VEGF seems to be required for induction of erythrocytosis and hepatic synthesis of *Epo*, as indicated by adenovirus titration studies, and dose-dependent effects with soluble VEGFRs and DC101. Such high-grade inhibition of VEGF is probably more optimally achieved by continuous and high-level adenoviral expression than by repetitive dosing of protein or small-molecule VEGF antagonists (**Supplementary Fig. 9** online), and is consistent with the slower and less robust erythrocytosis achieved with recombinant VEGF Trap versus adenoviral delivery. Recombinant VEGF Trap increased hematocrit in mice starting at doses of 2.5 mg/kg twice weekly and trough plasma levels of 20 μg/ml, with maximal erythrocytosis observed with higher and more frequent dosing (data not shown).

Data from studies using recombinant VEGF Trap protein or VEGFR2-specific antibody, a large panel of adenoviruses expressing non-VEGFR soluble receptors, parabiosis and intramuscular administration of adenovirus indicate that general hepatotoxicity does not underlie the observed hepatic synthesis of Epo and erythrocytosis. This is emphasized by the normal hepatocyte histology observed using treatment with Ad-sVEGFRs versus Ad-Fc or with VEGF Trap protein versus placebo. In addition, hepatocyte dropout and liver hemorrhage were not present with our conventional capsid adenoviruses, as previously noted for a sFlt1 adenovirus with a mutant capsid protein containing an RGD motif to enhance liver targeting through integrin interactions[35].

Hepatocyte-produced VEGF-A contributes to the ongoing repression of adult hepatic Epo production, based upon phenocopy of soluble VEGFR-stimulated erythrocytosis by Ad-Cre–mediated, hepatocyte-specific excision of a floxed *Vegfa* gene. As tyrosine kinase VEGFRs do not seem to be expressed on hepatocytes[32,34], an autocrine mechanism seems unlikely without invoking a receptor-independent mechanism or nonclassical VEGF receptors such as neuropilins; notably, a soluble neuropilin-1 ectodomain does not stimulate erythrocytosis. Alternatively, hepatocyte-produced VEGF could elicit paracrine stimulation of VEGFR2 on neighboring LSECs[32,34], followed by reciprocal endothelial repression of hepatocyte Epo production. VEGF-dependent endothelial repression could occur either through lack of a stimulatory factor or active production of an inhibitor (**Fig. 4f**). The former model is well supported by low basal production of *Epo* in hepatocyte monoculture, endothelial-dependent induction of hepatocyte *Epo* mRNA in coculture without exogenous VEGF and, conversely, its repression by VEGF.

Inhibition of VEGF stimulates hepatic synthesis of *Epo* through selective interference with VEGFR2-dependent endothelium-hepatocyte cross-talk, based upon several lines of evidence. A specific functional role for VEGFR2 is supported by both the ability of the VEGFR2-specific monoclonal antibody DC101 to induce erythrocytosis *in vivo* as well as repression of Epo in coculture by VEGF-A but not by the VEGFR1-selective ligand PlGF. In such a model, *in vivo* blockade of VEGF by either sVEGFRs, Cre-mediated *Vegfa* gene deletion or DC101 actively promotes inductive paracrine signaling from LSEC to hepatocytes, activating transcription of *Epo* with subsequent erythrocytosis. Consistent with the involvement of the hepatocyte-endothelium interface, we have observed adult sinusoidal remodeling with loss of fenestrae after blockade of VEGF (K.W. & C.J.K., unpublished data). Ample precedent for such endothelium-hepatocyte cross-talk exists during liver organogenesis[36] and regulation of adult hepatocyte proliferation by VEGF[30]. Notably, in the latter case[30] as well as here, endothelium-hepatocyte cross-talk seems to utilize specialized properties of the hepatic endothelium.

Hepatic production of *Epo* seems to be insensitive to *Hif1a* gene deletion and Ad-sVEGFR–treated livers did not show prominent indications of hypoxia. On the other hand, we cannot formally exclude either hypoxia or the potential involvement of other HIF family members such as HIF-1β and HIF-2α, which have been strongly implicated in hypoxia-induced hepatic expression of Epo[37–40], and whose potential roles are under active investigation.

To our knowledge, a relationship between VEGF and adult RBC homeostasis has not been previously described. In mice, adenoviral overexpression of VEGF or PlGF was reported to elevate WBC counts, CFU-GM and colony-forming units–megakaryocyte (CFU-M), although effects on RBC numbers were not reported[41,42]. Inhibition of VEGF by recombinant Flt1-Fc in neonatal mice was shown to produce mild increases in hematocrit, which were attributed to hypoxemia from heart-lung hypoplasia[31], which is not applicable here. Moreover, it was reported that treatment of adult mice with either a mouse VEGF-specific antibody or mouse Flt1-IgG fusion protein does not increase hematocrit[43], and erythrocytosis has not been reported in human clinical trials of either VEGF Trap or bevacizumab at conventional doses[3,4,44]. Nevertheless, our studies clearly showed robust erythrocytosis resulting from diverse methods of VEGF inhibition, including soluble receptors, VEGFR2-specific antibody and *Vegfa* gene deletion. Recombinant VEGF Trap increased hematocrit in cynomolgus monkeys, suggesting conservation of this mechanism across species, whereas in humans the small-molecule VEGF inhibitor SU5416 increases hematocrit in a limited subset of individuals with hemangioblastoma and Von Hippel–Lindau disease[45].

Potentially, the erythroid response observed here might be restricted to sVEGFRs and VEGFR-specific antibodies, which can antagonize multiple VEGF family members, as compared to other classes of VEGF antagonists with distinct mechanisms of action, such as VEGF-A–specific monoclonal antibodies or small-molecule inhibitors of tyrosine kinase VEGFRs. In addition, stringent inhibition of VEGF seems to be required for substantial increases in hematocrit, as greatly facilitated here by adenoviral delivery and the pharmacokinetics of VEGF Trap. With regard to the relevance of these findings to humans, we cannot exclude differential species susceptibility, as the maximum induction of erythrocytosis at equivalent VEGF Trap trough plasma levels was greater in mice than in primates. Notably, monkeys seem

less responsive than mice to identical weight-dosed administration of recombinant darbepoetin (G. Molineux, personal communication). Together, the current results suggest that erythrocytosis in humans could in fact be observed with higher dose intensities of VEGF inhibitors, particularly in individuals whose treatment does not include confounding factors such as simultaneous chemotherapy.

Overall, our studies indicate that VEGF acts as a novel physiological regulator of both adult erythropoiesis and synthesis of *Epo*, with inhibition of VEGF inducing normally dormant adult hepatic expression of *Epo* through interference with VEGF-A– and VEGFR2-dependent endothelial-hepatocyte cross-talk. Further evaluation of this circuit within the context of Epo transcriptional regulatory factors, the well-documented but poorly understood developmental switch between hepatic and renal *Epo* synthesis[21] and the potential role of hepatic Epo in modulating liver physiology or as a cytoprotective factor in the liver seems warranted. In the clinical setting, whether the high degree of VEGF blockade associated with erythrocytosis in the current studies would be either safe or desirable remains to be seen. Nonetheless, the recognition and clinical monitoring of erythrocytosis as a surrogate marker for stringent inhibition of VEGF is relevant to the numerous VEGF-targeted agents currently in dose-escalation clinical trials. Accordingly, the documentation of erythrocytosis or amelioration of anemia during clinical VEGF blockade would be of considerable interest, as would the establishment of correlations between erythrocytic endpoints and optimal antitumor dose intensities of VEGF antagonists such as soluble receptors.

METHODS

Construction and purification of adenoviruses. We constructed and purified the Ad-Flk1-Fc (entire mouse Flk1 ectodomain fused to IgG2α Fc), Ad-Fc (encoding IgG2α Fc) and Ad-NRP1 (encoding a neuropilin-1 ectodomain) as previously described[6]. Ad-HA-Flt1-His is identical to a previously described adenovirus expressing Flt1 (ref. 6), except for an N-terminal IgK signal peptide and hemagglutinin epitope. Ad-mac Epo expresses the entire open reading frame of the gene encoding macaque erythropoietin and is biologically active in mice (J.-S.L. & R.C.M., unpublished data). Ad-Cre recombinase was generated at the University of Iowa Gene Transfer Vector Core. Ad-EpoR-Fc and Ad-PDGFRβ expressing their cognate soluble ectodomains will be described separately (B.T. & C.J.K., unpublished data; F. Kuhnert & C.J.K., unpublished data). Ad-VEGF Trap expressing the fusion protein of the VEGF binding domains of Flt1 and Flk1 and human immunoglobulin domain[8] was generated using codon-optimized cDNA synthesized according to the VEGF Trap amino acid sequence.

Transgenic mice. *Hif1a*$^{loxP/loxP}$ mice with *lox*P sites flanking exon 2 of the *Hif1a* gene have been previously described[46]. *Vegfa*$^{loxP/loxP}$ mice with *lox*P sites flanking the second exon of the *Vegfa* gene were provided by H.P. Gerber and N. Ferrara (Genentech)[31]. The *Rosa26-LacZ* strain has been described previously and was provided by P. Soriano (Fred Hutchinson Cancer Research Center)[26].

Adenoviral injections and quantification of plasma sVEGFR levels. We injected 10–16-week-old C57BL/6 mice with 10^5–10^9 p.f.u. of the indicated adenoviral vector through the tail vein. After 2–3 d, retro-orbital acquisition of plasma samples and expression of Flk1-Fc and Flt1 were performed as previously described[6]. We determined levels of VEGF Trap by sandwich ELISA with capture by recombinant human $VEGF_{165}$ ($rhVEGF_{165}$; Peprotech), and detected them with a human Fc-HRP–specific antibody (NEN). All mice were housed and handled according to Stanford University Administrative Panel on Laboratory Animal Care guidelines.

Administration of pharmacologic VEGF inhibitors. Mice with severe combined immunodeficiency (SCID) received VEGF Trap protein subcutaneously two to three times per week at doses of 2.5–25 mg/kg as described in the text. At appropriate time points, blood was withdrawn by cardiac puncture. We measured levels of circulating free VEGF Trap by sandwich ELISA using $rhVEGF_{165}$ (Regeneron) as a capture reagent and a human Fc-HRP–specific antibody (Sigma) for detection. For control groups, we left mice untreated (0 mg/kg) or treated them with a vehicle solution of 5 mM sodium phosphate, 5 mM sodium citrate, 100 mM sodium chloride, 0.1% (wt/vol) polysorbate 20 and 20% (wt/vol) sucrose, pH 6.0. All mice and monkey protocols were approved by the Regeneron Institutional Animal Care and Use Committee.

Male cynomolgus monkeys received twice-weekly subcutaneous injections of VEGF Trap with 15 mg/kg or 30 mg/kg (30 or 60 mg/kg weekly cumulative dose, respectively) for 13 weeks. We collected blood from the saphenous, femoral or cephalic vein using a butterfly infusion set followed by determination of complete blood count (CBC).

DC101 (a rat IgG1 monoclonal antibody targeting mouse VEGFR2) was isolated from conditioned media of the cognate hybridoma ATCC HB-11534) by protein G affinity chromatography[15]. SCID mice received twice-weekly subcutaneous injections of DC101 at 40 mg/kg for 8 weeks followed by determination of CBC. We synthesized the small-molecule VEGFR inhibitor ZD4190 according to published methods and administered it by oral gavage at 100 mg/kg/d for 8 d[17,47].

Determination of hematocrit, CBC and reticulocytes. We determined spun hematocrit by centrifugation of whole blood in heparinized capillary tubes using the AutocritUltra3 (Clay Adams; **Supplementary Methods** online).

Determination of RBC mass. We determined RBC mass of Ad-Flt1–treated mice by biotinylation of RBCs (**Supplementary Methods**).

Analysis of erythroid precursors and CFU-E assays. We determined $Ter119^+CD45^-$ erythroid precursors in the bone marrow and spleen, and performed CFU-E progenitor assays (**Supplementary Methods**).

Cornea micropocket assay. We performed the VEGF-mediated cornea micropocket assay as previously described with corneal implantation of $rhVEGF\text{-}A_{165}$ hydron pellets[6] (**Supplementary Methods**).

Erythropoietin ELISA. We determined plasma erythropoietin levels (mU/ml) as described previously[18] or with a mouse Epo immunoassay kit (R&D Systems; **Supplementary Methods**).

Determination of gene expression and excision frequencies. Quantification of mouse and rat *Epo* mRNA is described in **Supplementary Methods**. We performed real-time PCR quantification of the *Hif1a*-regulated genes *Slc2a1* and *Pgk1* as previously described[29]. We determined the degree of excision of *Hif1a* and *Vegfa* in Ad-Cre–treated livers of *Hif1a*$^{loxP/loxP}$ and *Vegfa*$^{loxP/loxP}$ by real-time PCR using primers as described previously[29,48].

Nuclear run-on assay, parabiotic experiments, detection of EF-5 by immunohistochemistry and *in situ* hybridization. Details are in **Supplementary Methods**.

Isolation and culture of rat hepatocytes and LSECs. We isolated rat hepatocytes after *in situ* collagenase liver perfusion using a modification of a previously described technique[49] (**Supplementary Methods**).

For coculture studies, we prepared individual hepatocyte and LSEC cultures by separately plating each cell type onto type I collagen–coated plastic dishes (Bio-Coat, BD Biosciences) at a density of 1.0×10^5 cells/cm^2. We rinsed monolayers after 1 h to remove nonadherent cells. We prepared cocultures by plating hepatocytes as above and adding LSECs in a 1:1 ratio after 1 h. We added HUVECs, MS1 mouse pancreatic endothelial cells or mouse embryonic fibroblasts to the hepatocyte monolayers similarly in a 1:1 ratio for control coculture experiments. We treated hepatocyte-LSEC cocultures with 20 ng/ml of $rhVEGF\text{-}A_{165}$ or PlGF (R&D Systems) as indicated or left them untreated, with daily replenishment of treatments for 2 d. We harvested cells from each of the treatment groups for the isolation of total RNA on day 3. We performed real-time PCR quantification of *Epo* mRNA as described above.

Note: Supplementary information is available on the Nature Medicine website.

ACKNOWLEDGMENTS

We thank members of the Kuo laboratory for discussion, J. Folkman for support of this project, C. Davis for histopathologic analysis of liver sections, C.-P. Chang

for HA-Flt1-His cDNA, A. Patterson for determination of arterial oxygen tension, A. Wagers for demonstrating parabiotic surgeries, M. Socolovsky for murine Epo, J. Zehnder for advice with real-time PCR, C. Koch for EF5 and EF5-specific antibodies, G. Molineux for permission to cite unpublished data and E. Yu for initial assistance. We are indebted to H.-P. Gerber and N. Ferrara for their gift of *Vegfa*$^{loxP/loxP}$ mice, Y.-M. Lin and T. Wandless for synthesis of ZD4190 and the UCSF Liver Center (supported by NIH P30 DK26743) for providing core services. B.Y.Y.T. is a Fonds de la Recherche en Santé du Québec fellow. K.W. is supported by a Medical Scientist Training Program Grant to Stanford University. This work was supported by grants from the US National Institutes of Health (1 R01 CA95654-01 and 1 R01 HL074267-01) and the Department of Defense (DAMD17-02-1-0143) to C.J.K. and funds from Amgen Corporation (to R.J.K.). C.J.K. is a Burroughs Wellcome Foundation Scholar in the Pharmacological Sciences and a Kimmel Foundation Scholar.

AUTHOR CONTRIBUTIONS

B.Y.Y.T. and K.W. designed and performed experiments and wrote the manuscript. J.S.R. performed animal studies with VEGF Trap protein and edited the manuscript. J. Hoffman performed *Epo* RT-QPCR. J.Y. and C.C. generated Ad VEGF Trap and Ad KDR-Fc. G.W. assisted on hematocrit and flow cytometry studies. L.M. and S.L.S. analyzed RBC precursors. U.S. performed pathologic analysis. J. Holash and S.J. performed animal studies with VEGF Trap protein. S.K.P. performed studies with *Vegfa*$^{loxP/loxP}$ mice and RT-QPCR of hypoxic genes. R.S.J. and J.A.G. provided expertise in liver physiology. F.A.K. designed and performed RBC mass analysis. G.D.Y. supervised VEGF Trap studies. R.C.M. supervised adenoviral construction and production. C.J.K. was principal investigator, designed and conceptualized the study, analyzed and interpreted all data, and drafted and edited the manuscript.

COMPETING INTERESTS STATEMENT

The authors declare competing financial interests (see the *Nature Medicine* website for details).

Published online at http://www.nature.com/naturemedicine/
Reprints and permissions information is available online at http://npg.nature.com/reprintsandpermissions/

1. Ferrara, N., Gerber, H.P. & LeCouter, J. The biology of VEGF and its receptors. *Nat. Med.* **9**, 669–676 (2003).
2. Yancopoulos, G.D. *et al.* Vascular-specific growth factors and blood vessel formation. *Nature* **407**, 242–248 (2000).
3. Hurwitz, H. *et al.* Bevacizumab plus irinotecan, fluorouracil, and leucovorin for metastatic colorectal cancer. *N. Engl. J. Med.* **350**, 2335–2342 (2004).
4. Konner, J. & Dupont, J. Use of soluble recombinant decoy receptor vascular endothelial growth factor trap (VEGF Trap) to inhibit vascular endothelial growth factor activity. *Clin. Colorectal Cancer* **2**, S81–S85 (2004).
5. Ferrara, N. *et al.* Heterozygous embryonic lethality induced by targeted inactivation of the VEGF gene. *Nature* **380**, 439–442 (1996).
6. Kuo, C.J. *et al.* Comparative evaluation of the antitumor activity of antiangiogenic proteins delivered by gene transfer. *Proc. Natl. Acad. Sci. USA* **98**, 4605–4610 (2001).
7. Laird, A.D. *et al.* SU6668 inhibits Flk-1/KDR and PDGFRbeta in vivo, resulting in rapid apoptosis of tumor vasculature and tumor regression in mice. *FASEB J.* **16**, 681–690 (2002).
8. Holash, J. *et al.* VEGF-Trap: a VEGF blocker with potent antitumor effects. *Proc. Natl. Acad. Sci. USA* **99**, 11393–11398 (2002).
9. Maynard, S.E. *et al.* Excess placental soluble fms-like tyrosine kinase 1 (sFlt1) may contribute to endothelial dysfunction, hypertension, and proteinuria in preeclampsia. *J. Clin. Invest.* **111**, 649–658 (2003).
10. Eremina, V. *et al.* Glomerular-specific alterations of VEGF-A expression lead to distinct congenital and acquired renal diseases. *J. Clin. Invest.* **111**, 707–716 (2003).
11. Jacobi, J. *et al.* Discordant effects of a soluble VEGF receptor on wound healing and angiogenesis. *Gene Ther.* **11**, 302–309 (2004).
12. Zelzer, E. *et al.* VEGFA is necessary for chondrocyte survival during bone development. *Development* **131**, 2161–2171 (2004).
13. Levine, R.J. *et al.* Circulating angiogenic factors and the risk of preeclampsia. *N. Engl. J. Med.* **350**, 672–683 (2004).
14. Kuo, C.J., Farnebo, E.Y., Becker, C.M. & Folkman, J. VEGF-targeted antiangiogenic gene therapy. in *Gene Therapy of Cancer* (ed. Lattime, E.) (2002).
15. Prewett, M. *et al.* Antivascular endothelial growth factor receptor (fetal liver kinase 1) monoclonal antibody inhibits tumor angiogenesis and growth of several mouse and human tumors. *Cancer Res.* **59**, 5209–5218 (1999).
16. Fiedler, W. *et al.* A phase 2 clinical study of SU5416 in patients with refractory acute myeloid leukemia. *Blood* **102**, 2763–2767 (2003).
17. Wedge, S.R. *et al.* ZD4190: an orally active inhibitor of vascular endothelial growth factor signaling with broad-spectrum antitumor efficacy. *Cancer Res.* **60**, 970–975 (2000).
18. Rinaudo, D. & Toniatti, C. Sensitive ELISA for mouse erythropoietin. *Biotechniques* **29**, 218–220 (2000).
19. Gerber, H.P. *et al.* VEGF regulates haematopoietic stem cell survival by an internal autocrine loop mechanism. *Nature* **417**, 954–958 (2002).
20. Ziegler, B.L. *et al.* KDR receptor: a key marker defining hematopoietic stem cells. *Science* **285**, 1553–1558 (1999).
21. Ebert, B.L. & Bunn, H.F. Regulation of the erythropoietin gene. *Blood* **94**, 1864–1877 (1999).
22. Ryan, H.E., Lo, J. & Johnson, R.S. HIF-1 alpha is required for solid tumor formation and embryonic vascularization. *EMBO J.* **17**, 3005–3015 (1998).
23. Stec, D.E., Davisson, R.L., Haskell, R.E., Davidson, B.L. & Sigmund, C.D. Efficient liver-specific deletion of a floxed human angiotensinogen transgene by adenoviral delivery of Cre recombinase *in vivo*. *J. Biol. Chem.* **274**, 21285–21290 (1999).
24. Hegenbarth, S. *et al.* Liver sinusoidal endothelial cells are not permissive for adenovirus type 5. *Hum. Gene Ther.* **11**, 481–486 (2000).
25. Tao, N. *et al.* Sequestration of adenoviral vector by Kupffer cells leads to a nonlinear dose response of transduction in liver. *Mol. Ther.* **3**, 28–35 (2001).
26. Soriano, P. Generalized lacZ expression with the ROSA26 Cre reporter strain. *Nat. Genet.* **21**, 70–71 (1999).
27. Michael, M.D. *et al.* Loss of insulin signaling in hepatocytes leads to severe insulin resistance and progressive hepatic dysfunction. *Mol. Cell* **6**, 87–97 (2000).
28. Laughlin, K.M. *et al.* Biodistribution of the nitroimidazole EF5 (2-[2-nitro-1H-imidazol-1-yl]-N-(2,2,3,3,3-pentafluoropropyl) acetamide) in mice bearing subcutaneous EMT6 tumors. *J. Pharmacol. Exp. Ther.* **277**, 1049–1057 (1996).
29. Cramer, T. *et al.* HIF-1alpha is essential for myeloid cell-mediated inflammation. *Cell* **112**, 645–657 (2003).
30. LeCouter, J. *et al.* Angiogenesis-independent endothelial protection of liver: role of VEGFR-1. *Science* **299**, 890–893 (2003).
31. Gerber, H.P. *et al.* VEGF is required for growth and survival in neonatal mice. *Development* **126**, 1149–1159 (1999).
32. Jakeman, L.B., Winer, J., Bennett, G.L., Altar, C.A. & Ferrara, N. Binding sites for vascular endothelial growth factor are localized on endothelial cells in adult rat tissues. *J. Clin. Invest.* **89**, 244–253 (1992).
33. Maharaj, A.S., Saint-Geniez, M., Maldonado, A.E. & D'Amore, P.A. Vascular endothelial growth factor localization in the adult. *Am. J. Pathol.* **168**, 639–648 (2006).
34. Yamane, A. *et al.* A new communication system between hepatocytes and sinusoidal endothelial cells in liver through vascular endothelial growth factor and Flt tyrosine kinase receptor family (Flt-1 and KDR/Flk-1). *Oncogene* **9**, 2683–2690 (1994).
35. Mahasreshti, P.J. *et al.* Intravenous delivery of adenovirus-mediated soluble FLT-1 results in liver toxicity. *Clin. Cancer Res.* **9**, 2701–2710 (2003).
36. Matsumoto, K., Yoshitomi, H., Rossant, J. & Zaret, K.S. Liver organogenesis promoted by endothelial cells prior to vascular function. *Science* **294**, 559–563 (2001).
37. Hu, C.J., Wang, L.Y., Chodosh, L.A., Keith, B. & Simon, M.C. Differential roles of hypoxia-inducible factor 1alpha (HIF-1alpha) and HIF-2alpha in hypoxic gene regulation. *Mol. Cell. Biol.* **23**, 9361–9374 (2003).
38. Warnecke, C. *et al.* Differentiating the functional role of hypoxia-inducible factor (HIF)-1alpha and HIF-2alpha (EPAS-1) by the use of RNA interference: erythropoietin is a HIF-2alpha target gene in Hep3B and Kelly cells. *FASEB J.* **18**, 1462–1464 (2004).
39. Wiesener, M.S. *et al.* Widespread hypoxia-inducible expression of HIF-2alpha in distinct cell populations of different organs. *FASEB J.* **17**, 271–273 (2003).
40. Rankin, E.B., Tomaszewski, J.E. & Haase, V.H. Renal cyst development in mice with conditional inactivation of the von Hippel-Lindau tumor suppressor. *Cancer Res.* **66**, 2576–2583 (2006).
41. Hattori, K. *et al.* Vascular endothelial growth factor and angiopoietin-1 stimulate postnatal hematopoiesis by recruitment of vasculogenic and hematopoietic stem cells. *J. Exp. Med.* **193**, 1005–1014 (2001).
42. Hattori, K. *et al.* Placental growth factor reconstitutes hematopoiesis by recruiting VEGFR1(+) stem cells from bone-marrow microenvironment. *Nat. Med.* **8**, 841–849 (2002).
43. Malik, A.K. *et al.* Redundant roles of VEGF-B and PlGF during selective VEGF-A blockade in mice. *Blood* **107**, 550–557 (2006).
44. Lau, S.C., Rosa, D.D. & Jayson, G. Technology evaluation: VEGF Trap (cancer), Regeneron/Sanofi-Aventis. *Curr. Opin. Mol. Ther.* **5**, 493–501 (2005).
45. Richard, S. *et al.* Paradoxical secondary polycythemia in von Hippel-Lindau patients treated with anti-vascular endothelial growth factor receptor therapy. *Blood* **99**, 3851–3853 (2002).
46. Ryan, H.E. *et al.* Hypoxia-inducible factor-1alpha is a positive factor in solid tumor growth. *Cancer Res.* **60**, 4010–4015 (2000).
47. Hennequin, L.F. *et al.* Design and structure-activity relationship of a new class of potent VEGF receptor tyrosine kinase inhibitors. *J. Med. Chem.* **42**, 5369–5389 (1999).
48. Schipani, E. *et al.* Hypoxia in cartilage: HIF-1alpha is essential for chondrocyte growth arrest and survival. *Genes Dev.* **15**, 2865–2876 (2001).
49. Irving, M.G., Roll, F.J., Huang, S. & Bissell, D.M. Characterization and culture of sinusoidal endothelium from normal rat liver: lipoprotein uptake and collagen phenotype. *Gastroenterology* **87**, 1233–1247 (1984).